Polaronic Signatures in Mid-Infrared Spectra: Prediction for $LaMnO_3$ and $CaMnO_3$

Yiing-Rei Chen[1], Vasili Perebeinos[2] and Philip B. Allen[1]
[1] *Department of Physics and Astronomy, State University of New York, Stony Brook, New York 11794-3800*
[2] *Department of Physics, Brookhaven National Laboratory, Upton, New York 11973-5000*
(February 1, 2008)

Hole-doped $LaMnO_3$ and electron-doped $CaMnO_3$ form self-trapped electronic states. The spectra of these states have been calculated using a two orbital (Mn e_g Jahn-Teller) model, from which the non-adiabatic optical conductivity spectra are obtained. In both cases the optical spectrum contains weight in the gap region, whose observation will indicate the self-trapped nature of the carrier states. The predicted spectra are proportional to the concentration of the doped carriers in the dilute regime, with coefficients calculated with no further model parameters.

I. INTRODUCTION

Qualitative discussions of optical absorption from polarons [1] have often been given. For the heavily doped manganites such as $La_{0.7}Ca_{0.3}MnO_3$, polarons form at temperatures $T \geq T_c \approx 250$K where ferromagnetic order is lost. Dramatic thermal shifts of optical conductivity [2] agree [3] with the qualitative polaron picture [4]. In the lightly doped end-member compounds $LaMnO_3$ and $CaMnO_3$, polarons must exist at low temperature in the spin and orbitally ordered states. We have previously [5–9] calculated the properties of these polarons in the Mn e_g Jahn-Teller (MEJT) [10] model. Here we point out that the polarons have a rich spectrum of local excited states. We provide a quantitative calculation of the corresponding polaron-induced mid-infrared absorption. The transitions between these local levels are broadened by the Franck-Condon effect since each local level prefers its own rearrangement of the lattice. This is a general phenomenon expected in many insulators and may account for mid-infrared absorption in other systems as well [11].

In the usual theory of small polaron absorption [1,12], an electron is trapped at a single site in a non-degenerate orbital. The photon permits a transfer of the electron to a first neighbor site. Direct transfer to the gound state first neighbor polaron (corresponding to dc conductivity) is exponentially suppressed by unfavorable vibrational overlap ("Huang-Rhys") factors. The largest vibrational overlap is for transitions into states whose maximum amplitude overlaps with the zero-point motion of the distorted polaron on the original site. A Gaussian envoelope of Franck-Condon vibrational sidebands is predicted. The cases considered here differ in three ways. (1) Our electron levels are doubly degenerate before distortion. (2) Hund's energy is large which blocks hopping unless the neighbor atom has spin ferromagnetically aligned. (3) Our polarons are not strictly confined to a single site, and consequently have localized excited states in the self-organized potential well. These complications are not all unique to manganites, and should affect polaronic absorption in other materials as well.

Pure $LaMnO_3$ has a single Mn d electron in the e_g doublet ($\psi_2 = (x^2-y^2)/\sqrt{3}, \psi_3 = 3z^2-r^2$). Therefore there is a cooperative Jahn-Teller effect resulting in orbital ordering. The peak [13,14] near 2 eV in $\sigma(\omega)$ is interpreted [14,8] as $e_g \rightarrow e_g$ transitions across the Jahn-Teller (JT) gap. Pure $CaMnO_3$ has no e_g states occupied, and $\sigma(\omega)$ peaks at 3.6 eV [14] due to excitations across the gap between occupied (O $2p$ and Mn $t_{2g\uparrow}$) states and empty (Mn $e_{g\uparrow}$) states. These materials are insulating antiferromagnets (AF) with the nice property of being continuously dopable. Here we focus on two cases, $x = 1-\epsilon$ (electron-doped $CaMnO_3$) and $x = \epsilon$ (hole-doped $LaMnO_3$.) Both materials are insulators when pure, and remain so when lightly doped because of polaron formation.

We use the model Hamiltonian $\mathcal{H}_{\rm MEJT} = \mathcal{H}_t + \mathcal{H}_{\rm ep} + \mathcal{H}_{\rm L} + \mathcal{H}_U$ [5] [6] similar to the one used by Millis [10], except that we have $U = \infty$ for $LaMnO_3$. For $CaMnO_3$ we include also the t_{2g} AF exchange term $\mathcal{H}_J$ and do not need the Hubbard U term for dilute doping. Two e_g orbitals per Mn atom are kept to fully represent the symmetries of the orbitals and the crystal, and to drive JT distortions. In the hopping term

$$\mathcal{H}_t = \sum_{l,\pm,\alpha\beta} \sum_{\delta=x,y,z} t_{\alpha\beta}(\pm\hat{\delta}) c^\dagger_\alpha(\vec{l} \pm \hat{\delta}) c_\beta(\vec{l}), \qquad (1)$$

there is only one parameter, namely, the nearest-neighbor $t = (dd\sigma)$ integral from Slater-Koster two-center theory. In the electron-phonon interaction, we include both the oxygen breathing vibrations Q_1 and the local E_g-type oxygen motions (Q_2, Q_3) which give the Jahn-Teller distortion.

$$\mathcal{H}_{\rm ep} = -{\rm g} \sum_{\vec{l},\alpha\beta} c^\dagger_\alpha(\vec{l}) c_\beta(\vec{l}) (Q_3(\vec{l})\sigma^z_{\alpha\beta} + Q_2(\vec{l})\sigma^x_{\alpha\beta} + \sqrt{2} Q_1(\vec{l})\hat{I}_{\alpha\beta}). \qquad (2)$$

The indices α and β run though orbitals (ψ_2, ψ_3). $\mathcal{H}_L$ is the lattice elastic energy of oxygen displacement along Mn-O-Mn bond directions with an Einstein restoring force. Note that the JT modes $Q_\alpha(\vec{l})$ and $Q_\alpha(\vec{l}')$ are not independent when Mn sites $\vec{l}$ and $\vec{l}'$ are first neighbors, since the intervening oxygen is shared by both Mn atoms (this is called the "cooperative" phonon effect.)

At the $LaMnO_3$ end of the phase diagram, the dominant term of the Hamiltonian after electron-electron repulsion is $\mathcal{H}_{\rm ep}$. Instead of delocalizing in a conduction band, holes in lightly doped $LaMnO_3$ lower their energy more by self-trapping with local oxygen rearrangement, forming "anti-JT" small polarons [5]. At the $CaMnO_3$ end, at the cost of AF exchange energy, spin-flipping in the AF background allows the doped-in electron to lower its energy by delocalization. This spin-polaron effect competes with a localizing JT polaron effect from $\mathcal{H}_{\rm ep}$. The competition determines the size of the spin-lattice polaron [6].

In this work we calculate the excitation spectrum of the spin-lattice polaron in $CaMnO_3$ by Born-Oppenheimer approximation, and for $LaMnO_3$ we calculate the excitation spectrum of the self-trapped hole in a Cho-Toyozawa [15] approximation. Our non-adiabatic solutions allow us to calculate the Franck-Condon broadened optical excitation spectra of these lightly doped materials and predict new spectral features that should be experimentally visible.

II. SPIN-LATTICE POLARON SPECTRUM IN DOPED $CAMNO_3$

Undoped $CaMnO_3$ has $Mn^{4+}(t_{2g}^3)$ ions with $S = 3/2$ on an approximately simple cubic lattice, and bipartite (G type) AF order below $T_N = 125K$. One single doped-in electron will align with the $S = 3/2$ core spin by Hund coupling. Hopping to first neighbors is then blocked by the AF order. To reduce energy by delocalization, one Mn $S = 3/2$ atom flips. Then the nearby oxygens distort, to lift the e_g degeneracy. This gives a seven-site spin-lattice polaron [6]. The parameters were chosen to be $|t|/JS^2 = 158$, and $\Gamma = g^2/K|t| = 0.25$. Each of the seven Mn atoms provides two e_g orbitals to form a 14-dimensional Hilbert space in which the doped-in electron is partially delocalized.

The ground state of this polaron is calculated in adiabatic approximation. With the local oxygens distorted in the optimized pattern, the ground state lies in the gap with energy lowered from the e_g band by $-2.13|t|$. The remaining 13 excited states contain three dipole-allowed optical excitations. By re-optimizing the oxygen distortion pattern, these states (with original energies $1.20|t|$ and $1.93|t|$ above the e_g band) can have their energy lowered to sit below the e_g band by $-0.67|t|$. When the electron is optically excited to one of these states, oxygens do not have time to rearrange to a new optimal pattern, and therefore are left in a combination of vibrationally excited states with respect to the re-optimized oxygen pattern of the electronic excited state. The Franck-Condon principle therefore applies and gives vibrational sidebands. The energy level diagram is shown in Fig. 1.

To examine the optical spectrum of this seven-site polaron surrounded by 36 oxygens, we start from one of the three symmetry-equivalent electronic ground states $\psi_0(\vec{r}, \vec{u_0})$ (e.g., $\theta = 0$ [6]) with local lattice distortion $\vec{u_0} = (u_{0,1}, u_{0,2}, ..., u_{0,36})$ which minimize the energy $E_0(\vec{u})$ of the ground state. For distortions $\vec{u}$ near $\vec{u_0}$, the vibronic eigenstates associated with the electron ground state are approximated by the Born-Oppenheimer product:

$$\Psi_{0,n}(\vec{r}, \vec{u}) = \psi_0(\vec{r}, \vec{u_0}) \prod_{i=1}^{36} \phi_{i,n_i}(u_i - u_{0,i}), \qquad (3)$$

where $\phi_{i,n_i}(u_i - u_{0,i})$ is the n_i phonon state of the harmonic oscillator centered at $u_{0,i}$. The usual approximation is made here that $\psi_0(r, \vec{u})$ can be accurately represented by $\psi_0(r, \vec{u_0})$. The true electronic ground state varies slowly with $\vec{u}$, and also depends on the direction $\vec{u} - \vec{u_0}$ of deviation from $\vec{u_0}$, but corrections are small at low temperatures where the initial state is not vibrationally excited. Then the adiabatic ground state energy sheet $E_0(\vec{u})$ depends quadratically on $(\vec{u_i} - \vec{u_{0,i}})$ and we treat the oxygens as 36 independent Einstein oscillators, with energies

$$E_{0,n} = E_0(\vec{u_0}) + \hbar\omega \sum_{i=1}^{36} (n_i + \frac{1}{2}). \qquad (4)$$

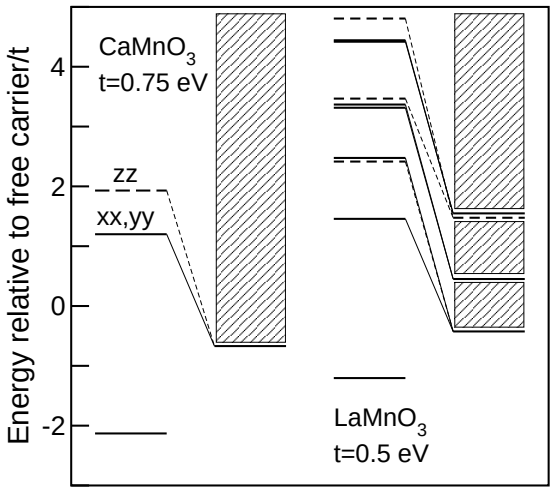

FIG. 1. Energy level diagrams for self-trapped states, relative to the lowest energy of a state in an undistorted environment. On the left are electron states in $CaMnO_3$ on the right are hole states in $LaMnO_3$. The lowest level is the ground state of the doped in e_g electron, bound by spin and lattice distortions. The dipole-allowed excited levels shown vertically keep the ground state distortions (dashed lines for $E||\hat{z}$ and solid lines for $E \perp \hat{z}$). Shown to the right are the relaxed energy levels corresponding to these excited states, and the shaded regions represent vibrational excitations accompanying the optical transitions.

Among the 13 polaronic excited states, there are only three states that couple to the ground state by light. They are $|\psi_z>\equiv(|\psi_3,\hat{z}>-|\psi_3,-\hat{z}>)/\sqrt{2}$ and two other states which are rotations of $|\psi_z>$ to $\hat{x}$ and $\hat{y}$ directions. Here $|\psi_3,\hat{z}>$ denotes the ψ_3 orbital of the Mn atom sitting immediately above the central Mn. These three excited states have their own optimal lattice distortion patterns $\vec{u_z}$, $\vec{u_x}$ and $\vec{u_y}$. Starting from $\vec{u_0}$, these electronic states remain eigenstates along the paths towards $\vec{u_z}$, $\vec{u_x}$ and $\vec{u_y}$ in the lattice distortion space. Therefore in these chosen directions, the vibronic eigenstates associated with the electronic excited states have the product form, e.g.:

$$\Psi_{z,n}(\vec{r},\vec{u})=\psi_z(\vec{r},\vec{u_z})\prod_{i=1}^{36}\phi_{i,n_i}(u_i-u_{z,i}). \tag{5}$$

Consider the optical excitation from Ψ_0 to Ψ_z for example. The $T=0$K spectrum is given by

$$\sigma^0(\omega)=\frac{\pi e^2N}{\Omega\hbar}\sum_{n'}|<f,n'|\hat{\epsilon}\cdot\vec{p}|i,0>|^2\,\delta(\frac{\Delta}{\hbar}+n'\omega_0-\omega) \tag{6}$$

The matrix element has both an electronic part and a phonon part. The electronic part involves the momentum matrix element $<\psi_z|p_z|\psi_3,0>$, where $|\psi_3,0>$ denotes the ψ_3 orbital of the central Mn atom. This matrix element is $<\psi_z|p_z|\psi_3,0>=ima/\hbar<\psi_z|\mathcal{H}_t|\psi_3,0>$, where m is the electron mass and a the lattice constant. This result can be derived by looking at FM spin order, and requiring that the corresponding FM Bloch eigenstates $|\vec{k}>$ of $\mathcal{H}_t$ (with energy $\epsilon(\vec{k})$) should have velocity $<\vec{k}|p_z/m|\vec{k}>=\partial\epsilon(\vec{k})/\partial\hbar k_z$.

The phonon part of the matrix element is $|<n',\vec{u_z}|n,\vec{u_0}>|^2$, where the initial lattice vibrational state has n vibrational quanta relative to the oxygen equilibrium positions $\vec{u_0}$. The lattice vibrational state is unchanged during the electron excitation, but must be expanded in the new basis (denoted by quanta n') around the new oxygen equilibrium positions $\vec{u_z}$. We consider only zero temperature optical conductivity, which restricts the initial vibrational quantum numbers n to be zero. The non-zero overlaps of this initial phonon state with the new phonon basis states of the displaced lattice give a spectrum with a Gaussian profile of delta function peaks of the multi-phonon transitions accompanying the electron exitation. The phonon frequency is taken to be $\hbar\omega=0.084$ eV. This is a little higher than the stretching frequency reported from Raman data [16], but the discrepancy does not affect our conclusions. The hopping integral t is taken from density-functional calculations [17] to be $t=-0.75$ eV. The delta functions are broadened into Gaussians of width $\sqrt{n'}\gamma$ where $\gamma=0.014eV$ and n' is the total vibrational quantum. The results are shown in Fig. 2.

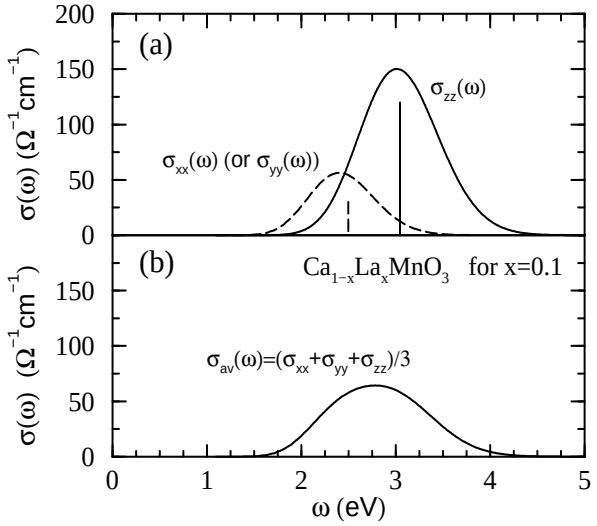

FIG. 2. Polaron-induced optical conductivity spectra of lightly doped $CaMnO_3$. (a) The dashed curve is for $E\perp\hat{z}$ and the solid line for $E\parallel\hat{z}$. Vertical lines present the adiabatic solution under fixed oxygen distortions and show the peaks at 2.50 eV and 3.05 eV. (b) In (a), the solutions belong to one of the possible ground states ($\theta=0$) [6]. There are two other possible ground states with orientations $\theta=2\pi/3$, and $\theta=4\pi/3$, which permute the directions $\hat{x}$, $\hat{y}$ and $\hat{z}$. Therefore we show the average spectrum. The absolute value of $\sigma(\omega)$ is shown for 10% electron doping.

III. POLARONIC SPECTRA IN HOLE DOPED $LAMNO_3$

In $LaMnO_3$ the electron-phonon term $\mathcal{H}_{\rm ep}$ stabilizes an orbitally ordered ground state *via* a cooperative JT oxygen distortion. We use the same model as in $CaMnO_3$, with different filling, and fit it to the JT ground state. We previously used this model to predict the resonant multiphonon Raman cross-section [9] and the angle resolved photoemission spectrum including the Franck-Condon broadening [7]. The photoemission process creates a sudden hole without time for oxygen relaxation. Thus it is in a vibrationally excited state. In the doped compound a hole is initially present in its ground vibrational state in a locally distorted oxygen environment. The zeroth order electronic many-body wave function has a hole h in the orbital at the origin 0 (taken arbitrarily to be an x-oriented orbital) in an otherwise perfectly correlated state with one E_g electron per atom.

$$\begin{aligned}|h0> &= c_X(0)|{\rm JT}>\\ |{\rm JT}> &= \prod_{\ell}^{A}c_X^\dagger(\ell)\prod_{\ell'}^{B}c_Y^\dagger(\ell')|0>\end{aligned} \tag{7}$$

Here the orbitals ψ_X and ψ_Y are orthogonal $x-$ and $y-$oriented orbitals $(\psi_2\pm\psi_3)/\sqrt{2}$.

At the next level of approximation the state $|h0>$ is coupled to 18 other states. Six of these states keep the

hole at the origin but have an orbital defect, or "orbiton" o on one of the surrounding Mn sites $\pm\hat{\ell}$ where $\hat{\ell}$ is $\hat{x}$, $\hat{y}$, or $\hat{z}$,

$$|h0, o \pm \hat{\ell} >= c_X^\dagger(\pm\hat{\ell}) c_Y(\pm\hat{\ell})|h0> \tag{8}$$

Six more states have the hole moved to the neighboring Mn site, with no orbital defect,

$$|h \pm \hat{\ell} >= c_Y(\pm\hat{\ell}) c_X^\dagger(0)|h0> . \tag{9}$$

The last six states have the hole on a neighbor and leave a misoriented $|Y>$ orbital at the origin,

$$|h \pm \hat{\ell}, o0 >= c_Y(\pm\hat{\ell}) c_Y^\dagger(0)|h0> . \tag{10}$$

The Hamiltonian $\mathcal{H}_{\rm MEJT}$ becomes a 19×19 matrix in this truncated Hilbert space.

In the adiabatic solution of the zeroth order hole ground state $|h0>$, the neighboring oxygens in $\pm\hat{x}, \pm\hat{y}, \pm\hat{z}$ directions are distorted to positions given in Table I, row 1, which minimize the polaron energy [5].

With the oxygen pattern frozen in these positions, the diagonal element $< h0|\mathcal{H}_{\rm ep}|h0>$ is set to zero. Nonzero Q_3 distortions on the neighboring sites couple the state $|h0>$ to the six orbital excitations $|h0, o \pm \hat{\ell}>$. Row 2 of Table I gives the diagonal elements $< h0, o \pm \hat{\ell}|\mathcal{H}_{\rm ep}|h0, o \pm \hat{\ell}>$ and row 3 gives the corresponding off-diagonal elements. The electron hopping term $\mathcal{H}_t$ couples the state $|h0>$ to states with the hole moved to the one of the six neighboring sites, both without (Eq. 9) and with (Eq. 10) an orbital defect. The energies of these states are given in Table I rows 4 and 5.

Diagonalization of this 19×19 matrix gives the ground state polaron solution and the excited spectra. Among the 18 excited states, there are 9 odd states which are coupled by light to the even parity ground state with momentum matrix elements $< \Psi|\hat{p}|h0 >= ima/\hbar < \Psi|\mathcal{H}_t|h0>$, whereas the other 9 even states are optically silent. No new parameter is needed for dipole matrix elements to predict the absolute value of $\sigma(\omega)$. The spectra would consist of 9 delta functions, three for E-field polarized in $\hat{z}$ direction $\sigma_\perp(\omega)$ and six for $\sigma_\parallel(\omega)$ shown by vertical lines on Fig. (3, a). The parameters were chosen to be $\Delta = 0.95$ eV, $t = 0.5$ eV, $\hbar\omega = 0.075$ eV, and Mn-Mn distance $a = 4.0\mathring{A}$.

In order to investigate the lattice-coupled electronic excitation, the surrounding oxygens should be allowed to vibrate. Since the frozen oxygen positions are not optimal for the excited hole states, Franck-Condon vibrational sidebands should appear in the optical spectrum. Assuming that the individual vibrational sidebands are not energy-resolved, there will be broadening by an amount roughly equal to the energy gain due to structural relaxation. In order to quantitatively describe the process, a theory beyond the adiabatic approximation is needed.

We use an approach similar to that applied to describe photoemission in the undoped material [7]. The method was proposed by Cho and Toyazawa [15], who used an infinitely large truncated Hilbert space to diagonalize a 1D polaronic Hamiltonian. For each of the states appearing in Eq. (8), Eq. (9) and Eq. (10), we re-optimize the positions of the 6 oxygens surrounding the hole. The relaxed energies are listed in Table I, row 6, 7, and 8. Notice that for each of the states in Eq. (8), the energy gain from relaxation is Δ, similar to exciton creation in the parent compound [8]. Each of these states, including $|h0>$, is now allowed to have arbitrary number of vibrational quanta of the surrounding oxygens around their re-optimized positions for that particular state. This adds additional vibrational multiples $n\hbar\omega$ to the relaxed energy. In this chosen basis, the $\mathcal{H}_{\rm ep} + \mathcal{H}_{\rm L}$ term of the Hamiltonian is diagonal. The complete Hamiltonian with the off-diagonal term $\mathcal{H}_{\rm t}$ can be diagonalized exactly. The hole ground state is not vibrationally excited at zero temperature, and the electronic part of this ground state has even symmetry which is coupled by light to odd excited states.

The Cho-Toyozawa calculation can be simplified by ignoring the sharing of the oxygens by its two nearest Mn neighbors. This partial removal of the "cooperative phonon" constraints was found in our photoemission calculation [7] to make only a small error. The energies of the odd parity states can be obtained as roots of the following analytic equation:

$$G_\ell^1(E)G_\ell^2(E) + G_\ell^1(E)G_\ell^3(E) = 1$$
$$G_\ell^i(E) = t_\ell^i \exp(-a_\ell^i) \sum_{n=0}^{\infty} \frac{1}{E - b_\ell^i - n} \frac{(a_\ell^i)^n}{n!} \tag{11}$$

The roots E give energies of the excited states for light polarized in $\ell = \hat{x}, \hat{y}, \hat{z}$ directions. The parameters a_ℓ^i, b_ℓ^i and t_ℓ^i in Eq. 11 are given in table I. The meaning of parameters a_ℓ^i is the energy gain due to the structural rearrangement. The parameters b_α^i are energies of the electronic excited states in vibrational ground state with relaxed oxygen distortions. The hopping matrix elements t_α^i couple the ground state to the electronically excited states and they are proportional to the dipole matrix elements of the allowed transitions. The parameters Δ and t used in Eq. 11 are all in units of $\hbar\omega = 75$ meV.

The energy of the ground state is lowered by 0.39 eV due to the hole delocalization on the neighboring sites such that only 83 % of the polaron is present on the central site. This value is very close to the estimation by second order perturbation theory [5], which gives $-0.167t/\Gamma - 0.488\Gamma t = 0.41$ eV ($\Gamma = \Delta/(8t)$). The excitation spectrum is measured from the renormalized ground state energy and shown on Fig. 3. It should be noted that the electronically excited states have their maximum weight on the neighboring sites and are not allowed to lower their energies by spreading on the next neighboring sites due to the truncation of the Hilbert space. We have done an estimate of the finite Hilbert space effect by comparing the adiabatic spectra using 19 electronic states on 7 sites with those from the 79 states on 27 sites

including the next neighboring atoms. The spectrum in a larger basis has been shifted by approximately 0.3 eV to lower energies. The energy peak positions and relative intensities in the adiabatic solution follow the trend of the non-adiabatic result (see Fig 3.a). We expect an overall shift of the spectrum in Fig. 3 to the lower energy by about 0.3 eV, such that the the spectrum sets in at about 0.7 eV.

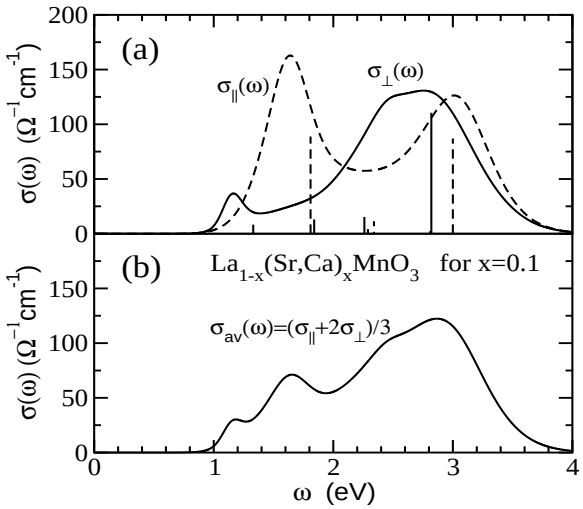

FIG. 3. Polaron-induced optical conductivity spectra of lightly doped $LaMnO_3$. (a) The dashed line is for $E \parallel \hat{z}$ and solid line for $E \perp \hat{z}$. Vertical lines is an adiabatic solution (frozen oxygen distortions). The non adiabatic spectra consist of three and six Franck-Condon broadened peaks for $E \parallel \hat{z}$ and $E \perp \hat{z}$ respectively. (b) Shows the average over polarizations. The overall spectral weight is proportional to the hole concentration and is given for 10% doping.

IV. CONCLUSION

The particular details for the manganites show that interesting processes occur which were not fully anticipated in the qualitative discussions previously given [1]. Similar processes should be at work in other insulators such as cuprates and nickelates.

New spectral features are predicted to appear in the JT gap of lightly doped $LaMnO_3$, and in the insulating gap of lightly doped $CaMnO_3$. The excitation spectra are calculated in non-adiabatic Born-Oppenheimer or Cho-Toyozawa approximation. These excitations are dipole-allowed with dipole matrix elements proportional to the hopping parameter t.

In the high T paramagnetic phase, in a mean field approximation, spin disorder has the effect of reducing the parameter t by 30%. This estimate suggests that the spectral weight due to hole excitations in $LaMnO_3$, for example, is reduced by 50% above the Néel temperature $T_N \approx 140K$ [18], whereas the orbiton excitation centered at 2 eV [8] is not sensitive to magnetic order and hence is temperature independent. In $CaMnO_3$, above $T_N \approx 125K$ [18], spin polarons should persist in disordered and increasingly delocalized form. This will cause the spectrum of Fig. 2 to broaden and shift to lower energy.

Our picture makes the prediction that, at frequencies well below the lowest weak peak in the sub-gap region, there should be a weak Urbach tail with characteristic Urbach temperature dependence. The tail is from the lowest-energy processes, and are weak because of small vibrational overlap. The available experimental data [14] on doped compounds agree with our picture. Further experiments on more lightly-doped materials, and especially transmission experiments through thin single crystals, would give a better test of our theory.

ACKNOWLEDGMENTS

This work was supported in part by NSF Grant No. DMR-0089492 and by DOE Grant No. DE-AC-02-98CH10886.

[1] D. Emin, Phys. Rev. B **48**, 13691 (1993).
[2] Y. Okimoto and Y. Tokura, J. Supercond. **13**, 271 (2000).
[3] K. H. Kim, J. H. Jung, and T. W. Noh, Phys. Rev. Lett **81**, 1517 (1998); S. G. Kaplan, M. Quijada, H. D. Drew, D. B. Tanner, G. C. Xiong, R. Ramesh, C. Kwon, and T. Venkatesan, Phys. Rev. Lett. **77**, 2081 (1996); H. L. Liu, S. L. Cooper, and S.-W. Cheong, Phys. Rev. Lett. **77**, 4684 (1998).
[4] A. J. Millis, P. B. Littlewood, and B. I. Shraiman, Phys. Rev. Lett. **74**, 5144 (1995); A. J. Millis, R. Mueller, and B. I. Shraiman, Phys. Rev. B **54**, 5405 (1996); S. Yunoki, A. Moreo, and E. Dagotto, Phys. Rev. Lett. **81**, 5612 (1998); A. S. Alexandrov and A. M. Bratkovsky, Phys. Rev. B **60**, 6215 (1999).
[5] P. B. Allen and V. Perebeinos, Phys. Rev. B **60**, 10747 (1999).
[6] Y. R. Chen and P. B. Allen, Phys. Rev. B **64**, 064401 (2001).
[7] V. Perebeinos and P. B. Allen, Phys. Rev. Lett. **85**, 5178 (2000).
[8] P. B. Allen and V. Perebeinos, Phys. Rev. Lett. **83**, 4828 (1999).
[9] V. Perebeinos and P. B. Allen, Phys. Rev. B **64**, 085118 (2001).
[10] A. J. Millis, Phys. Rev. B **53**, 8434 (1996).
[11] J. D. Perkins, J. M. Graybeal, M. A. Kastner, R. J. Birgeneau, J. P. Falck, and M. Greven, Phys. Rev. Lett. **71**, 1621 (1993); D. A. Crandles, T. Timusk, J. D. Garret, and J. E. Greedan, Physica C **216**, 94 (1993).

[12] A pedagogical discussion can be found at http://insti.physics.sunysb.edu∼allen/Polarons/MIR.html
[13] T. Arima, Y. Tokura, and J. B. Torrance, Phys. Rev. B **48**, 17006 (1993).
[14] J. H. Jung, K. H. Kim, D. J. Eom, T. W. Noh, E. J. Choi, J. Yu, Y. S. Kwon, and Y. Chung, Phys. Rev. B **55**, 15489 (1997); J. H. Jung, K. H. Kim, T. W. Noh, E. J. Choi, and J. Yu, Phys. Rev. B **57**, 11043 (1998).
[15] K. Cho and Y. Toyozawa, J. Phys. Soc. Jpn. **30**, 1555 (1971).
[16] E. Liarokapis, Th. Leventouri, D. Lampakis, D. Palles, J. J. Neumeier, and D. H. Goodwin, Phys. Rev. B **60**, 12758 (1999); E. Granado, N. O. Moreno, H. Martinho, A. Garcia, J. A. Sanjurjo, I. Torriani, C. Rettori, J. J. Neumeier, and S. B. Oseroff, Phys. Rev. Letters **86**, 5385 (2001).
[17] W. E. Pickett and D. J. Singh, Phys. Rev. B **53**, 1146 (1996).
[18] E. O. Wollan and W. C. Koehler, Phys. Rev. **100**, 545 (1955).

TABLE I. The parameters of the single-hole version of Hamiltonian $\mathcal{H}_{\rm MEJT}$ for oxygen displacements (row 1), the diagonal elements $< h0, o \pm \hat{\ell}|H|h0, o \pm \hat{\ell} >$ are shown in row 2, the off-diagonal coupling elements $gQ_3(\ell)$ are in row 3, the diagonal elements $< h \pm \hat{\ell}|H|h \pm \hat{\ell} >$ are in row 4, the diagonal elements $< h \pm \hat{\ell}, o0 > |H|h \pm \hat{\ell}, o0 >$ are in row 5. The relaxed energies of each of the states $|h0, o \pm \hat{\ell} >$ are in row 6, $|h \pm \hat{\ell} >$ are in row 7 and $|h \pm \hat{\ell}, o0 >$ are in row 8. The parameters a^i_ℓ, b^i_ℓ and t^i_ℓ $(i = 1, 2, 3)$ used in Eq. 11 are given in the rest of the table.

$\hat{\ell} =$	$\pm\hat{x}$	$\pm\hat{y}$	$\pm\hat{z}$
1	$\pm(\sqrt{4/3}-1)g/K$	$\mp(\sqrt{4/3}+1)g/K$	$\mp\sqrt{4/3}g/K$
2	$(7-2/\sqrt{3})\Delta/4$	$(7+2/\sqrt{3})\Delta/4$	2Δ
3	$(2\sqrt{2}+\sqrt{6})\Delta/24$	$(2\sqrt{2}-\sqrt{6})\Delta/24$	$-\sqrt{2}\Delta/6$
4	$37\Delta/24$	$37\Delta/24$	$40\Delta/24$
5	$61\Delta/24$	$61\Delta/24$	$64\Delta/24$
6	$(3-2/\sqrt{3})\Delta/4$	$(3+2/\sqrt{3})\Delta/4$	Δ
7	0	0	0
8	$(3+2/\sqrt{3})\Delta/4$	$(3-2/\sqrt{3})\Delta/4$	Δ
a^1_ℓ	Δ	Δ	Δ
a^2_ℓ	$37\Delta/24$	$37\Delta/24$	$40\Delta/24$
a^3_ℓ	$(43/3-4/\sqrt{3})\Delta/8$	$(43/3+4/\sqrt{3})\Delta/8$	$40\Delta/24$
b^1_ℓ	$(6-4/\sqrt{3})\Delta/8$	$(6+4/\sqrt{3})\Delta/8$	Δ
b^2_ℓ	0	0	0
b^3_ℓ	$(6+4/\sqrt{3})\Delta/8$	$(6-4/\sqrt{3})\Delta/8$	Δ
t^1_ℓ	$(2+\sqrt{3})t/4$	$(2-\sqrt{3})t/4$	$t/2$
t^2_ℓ	$(2+\sqrt{3})t/4$	$(2-\sqrt{3})t/4$	$t/2$
t^3_ℓ	$(2-\sqrt{3})t/4$	$(2+\sqrt{3})t/4$	$t/2$